

Gravitational lensing by a Bronnikov-Kim wormhole under a weak-field approximation and in a strong deflection limit

Naoki Tsukamoto^{1*}

¹*Department of General Science and Education,
National Institute of Technology,
Hachinohe College, Aomori 039-1192, Japan*

We consider gravitational lensing under a weak-field approximation and in a strong deflection limit by a Bronnikov-Kim wormhole with the same metric as the one of a wormhole filled with massless and neutral fermions in Einstein-Dirac-Maxwell theory. The metric approaches into the metric of an extreme charged Reissner-Nordström black hole in a black hole limit and it becomes the metric of an spatial Schwarzschild wormhole in an ultrastatic limit. In both of the black hole limit and the ultrastatic limit, the coefficient of a divergent term and the constant term of the deflection angle of a light in the strong deflection limit can be obtained exactly without expanding of parameters of the spacetime. Interestingly, in the both limits to the black hole and the ultrastatic wormhole, we obtain exactly the same coefficient and constant term in the strong deflection limit.

I. INTRODUCTION

Gravitational lensing under a weak-field approximation is a useful tool to find dark and massive objects [1, 2]. Recently, the direct observations of gravitational waves from compact objects have been reported by LIGO Scientific and Virgo Collaborations [3] and the shadow image of a supermassive black hole candidate at the center of galaxy M87 has been reported by Event Horizon Telescope Collaboration [4]. Gravitational lensing in a strong gravitational field by compact objects also can become an important tool to search them in future. Gravitational lensing in a strong deflection limit [5] is used to obtain observables by a light ray reflected by a photon sphere, which is a sphere formed by unstable circular light orbits, around a compact object [5–24]. The strong deflection limit analysis in the Schwarzschild spacetime was investigated by Bozza et al. [16] and its extensions and alternatives were investigated by several authors [5, 6, 20–46].

A wormhole is a hypothetical spacetime structure with non-trivial topology in general relativity [47] and it can be a black hole mimicker [48–50]. It is known that energy conditions are violated at the throat of the asymptotically flat, static, spherically symmetric wormhole at least if general relativity without a cosmological constant is assumed [51]. Many passable wormholes were suggested after an Ellis-Bronnikov wormhole [52–54]. In 2001, Dadhich *et al.* considered wormhole metrics with a vanishing Ricci scalar [55] and then Bronnikov and Kim also suggested wormhole metrics with a vanishing Ricci scalar in a braneworld scenario [56, 57]. Gravitational lensing by a spatial Schwarzschild wormhole with the vanishing Ricci scalar [55] in the strong deflection limit [5] has been investigated in Ref. [6].

Recently, a wormhole filled with massless and neutral fermions in Einstein-Dirac-Maxwell theory was obtained

numerically [58] and the existence of a thin shell at the wormhole throat is discussed in Refs. [59–62]. Its metric correspond with the Bronnikov-Kim wormhole as a simple and analytical metric case [56, 59, 60]. Its shadow size also have been investigated by Bronnikov *et al.* [63] and the orbit of a star around the wormhole have been investigated by Jusufi *et al.* [64]. Moreover, Churilova *et al.* [65] have discussed the shadow or the apparent sizes of photon spheres of the asymmetric wormhole [62] in a small asymmetry case.

On this paper, we consider gravitational lensing under the weak-field approximation and in the strong deflection limit by the Bronnikov-Kim wormhole [56, 57] with the same metric as the one of the wormhole filled with massless and neutral fermions in Einstein-Dirac-Maxwell theory [58]. The metric approaches into the metric of an extreme charged Reissner-Nordström black hole in a black hole limit and it does into the metric of the spatial Schwarzschild wormhole [55] in an ultrastatic limit.

This paper is organized as follows. The deflection angle of a ray in the Bronnikov-Kim wormhole spacetime is obtained in Sec. II, a lens equation is introduced in Sec. III, and observables under a weak-field approximation is obtained in Sec. IV. The deflection angle and observables in the strong deflection limit are investigated in Secs. V and VI, respectively and then we discuss and conclude our results in Sec VII. We investigate an Arnowitt-Deser-Misner (ADM) mass in appendix A and we review Schwarzschild lensing very briefly in appendix B. In this paper, we use the units in which the light speed and Newton’s constant are unity.

II. DEFLECTION ANGLE IN THE BRONNIKOV-KIM WORMHOLE SPACETIME

The line element of the Bronnikov-Kim wormhole spacetime [56, 57] is given by

$$ds^2 = -A(r)dt^2 + B(r)dr^2 + r^2(d\vartheta^2 + \sin^2\vartheta d\varphi^2), \quad (2.1)$$

* tsukamoto@rikkyo.ac.jp

where $A(r)$ and $B(r)$ are defined by

$$A(r) \equiv \left(1 - \frac{M}{r}\right)^2 \quad (2.2)$$

and

$$B(r) \equiv \frac{1}{\left(1 - \frac{r_+}{r}\right)\left(1 - \frac{r_-}{r}\right)} = \frac{1}{1 - \frac{2Q^2}{Mr} + \frac{Q^2}{r^2}}, \quad (2.3)$$

respectively, and where M and Q are positive constants which have been assumed $0 < M < Q$ and r_{\pm} are defined by

$$r_{\pm} \equiv \frac{Q^2}{M} \pm \sqrt{\frac{Q^4}{M^2} - Q^2}. \quad (2.4)$$

There is a wormhole throat at $r = r_+$. Note that $M/2 < r_- < M < r_+$. In a black hole limit $Q \rightarrow M$, the metric approaches into the metric of the extreme charged Reissner-Nordström black hole spacetime and we obtain $r_{\pm} = M = Q$. There are time translational and axial Killing vectors $t^{\mu}\partial_{\mu} = \partial_t$ and $\phi^{\mu}\partial_{\mu} = \partial_{\phi}$, since the spacetime has stationarity and axisymmetry, respectively. If the norm of the time translational Killing vector is a constant, the spacetime is called ultrastatic spacetime. Notice that a relation $M = 2Q^2r_+/(Q^2 + r_+^2)$. As shown in appendix A, an Arnowitt-Deser-Misner (ADM) mass m is given by

$$m = \frac{Q^2}{M}. \quad (2.5)$$

If we consider an ultrastatic limit $M \rightarrow 0$ under a fixed ADM mass m , we obtain the metric of an spatial Schwarzschild wormhole [6, 55] in the following form:

$$ds^2 = -dt^2 + \frac{dr^2}{1 - \frac{2m}{r}} + r^2(d\vartheta^2 + \sin^2\vartheta d\varphi^2), \quad (2.6)$$

which has a vanishing Ricci scalar while it has non-zero components of Ricci tensors. We can assume $\vartheta = \pi/2$ without loss of generality.

From $k^{\mu}k_{\mu} = 0$, where $k^{\mu} \equiv \dot{x}^{\mu}$ is the wave number and the overdot denotes a differentiation with respect to an affine parameter, the trajectory of a ray is given by

$$-A\dot{t}^2 + B\dot{r}^2 + r^2\dot{\varphi}^2 = 0 \quad (2.7)$$

and it can be expressed by $\dot{r}^2 + V(r)/E^2 = 0$, where $V(r)$ is an effective potential defined by

$$V(r) \equiv \frac{1}{Br^2} \left(b^2 - \frac{r^2}{A}\right), \quad (2.8)$$

where $b \equiv L/E$ is the impact parameter of the ray and $E \equiv -g_{\mu\nu}t^{\mu}k^{\nu} = A\dot{t}$, and $L \equiv g_{\mu\nu}\phi^{\mu}k^{\nu} = r^2\dot{\varphi}$ are the conserved energy and angular momentum of the light ray, respectively. We assume that L and b are positive unless we focus on negative ones. We assume that the closest distance of the light ray is $r = r_0$. Note that

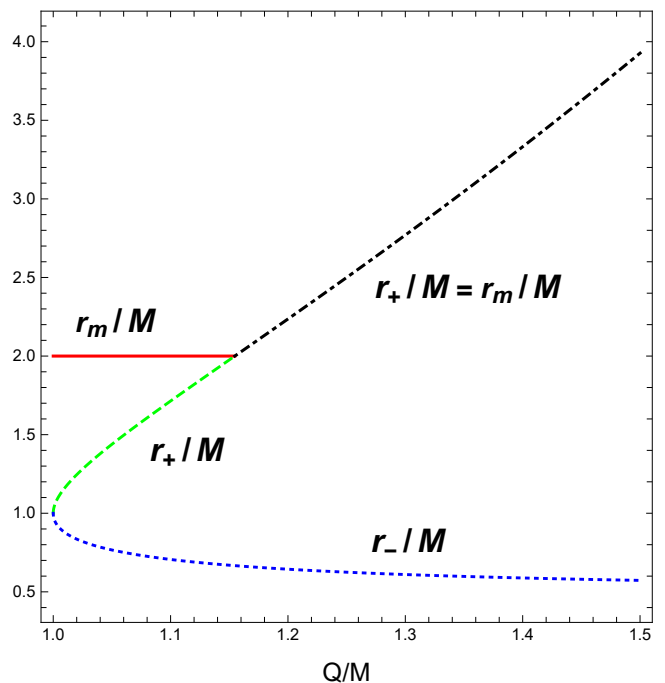


FIG. 1. The reduced radial coordinates of a photon sphere r_m/M , throat r_+/M , and r_-/M for given Q/M . A (red) solid line, a (green) dashed curve, a (blue) dotted curve, and a (black) dashed-dotted curve denote $r_m/M = 2$ for $1 < Q/M \leq 2/\sqrt{3}$, $1 < r_+/M \leq 2$ for $1 < Q/M \leq 2/\sqrt{3}$, $1/2 < r_-/M < 1$ for $1 < Q/M$, and $r_+/M = r_m/M$ for $2/\sqrt{3} \leq Q/M$, respectively.

$V_0 \equiv V(r_0) = 0$ holds. Here and hereinafter, any function with the subscript 0 denotes the function at the closest distance $r = r_0$. Light rays can exist in a region for $V(r) \leq 0$. For $1 < Q/M < 2/\sqrt{3}$, a ray with $b = b_m = 4M$ has $V_m = V'_m = 0$ and $V''_m < 0$ on the photon sphere at $r = r_m = 2M$ and the one with $b = r_+^2/(r_+ - M)$ has $V(r_+) = V'(r_+) = 0$ and $V''(r_+) > 0$ on the throat which works as an antiphoton sphere, which is sphere formed by stable circular light orbits, at $r = r_+$.¹ Here and hereinafter, the prime denotes the differentiation with respect to the radial coordinate r or the closest distance r_0 and functions with the subscript m denote the functions at $r = r_m$ or $r_0 = r_m$. For $Q/M > 2/\sqrt{3}$, the one with $b = b_m = r_+^2/(r_+ - M)$ has $V_m = V'_m = 0$ and $V''_m < 0$ on the throat to work as the photon sphere at $r = r_+ = r_m$. For a marginal case $Q/M = 2/\sqrt{3} \sim 1.1547$, the one with $b = b_m = 4M$ has $V_m = V'_m = V''_m = 0$ and $V'''_m = -4/M^3 < 0$ on the throat working as a marginally unstable photon sphere at $r = r_m = r_+ = 2M$. A light ray falls into the throat at $r = r_+$ for $b < b_m$, it rotates around the photon sphere

¹ It is concerned that stable circular light orbits may cause to instability of ultracompact objects because of the slow decay of linear waves [66–68].

at $r = r_m$ infinite times for $b = b_m$, and it is reflected by the throat for $b > b_m$. On this paper, we concentrate on light rays in the scattered case $b > b_m$ and gravitational lensing in a usual lens configuration.

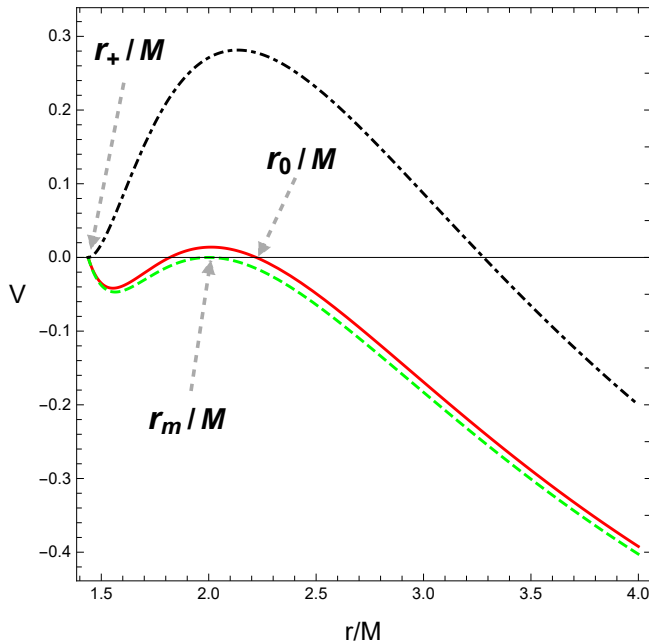


FIG. 2. Effective potentials V with $Q/M = 1.05$. A solid (red) curve denotes an effective potential V with $b/M = 1.01b_m/M = 4.04$ and $r_0/M = 2.22$, a dashed (green) curve denotes V with $b/M = b_m/m = 4.00$, and a dot-dashed (black) curve denotes V with $b/M = r_+^2/(r_+ - M) = 4.72$. Note $r_m/M = 2.00$ and $r_+/M = 1.44$.

From Eq. (2.7), we obtain

$$A_0 t_0^2 = r_0^2 \dot{\varphi}_0^2 \quad (2.9)$$

and the impact parameter of the light can be expressed as a function of r_0 ,

$$b(r_0) = \frac{L}{E} = \frac{r_0^2 \dot{\varphi}_0}{A_0 t_0} = \frac{r_0}{\sqrt{A_0}} = \frac{r_0^2}{r_0 - M}. \quad (2.10)$$

From the equation of the trajectory of the ray (2.7), the deflection angle of the ray is given by

$$\alpha = I(r_0) - \pi, \quad (2.11)$$

where $I(r_0)$ is defined as

$$I(r_0) \equiv 2 \int_{\infty}^{r_0} \frac{b dr}{r^2 \sqrt{-V(r)}}. \quad (2.12)$$

III. LENS EQUATION

We assume that an observer O and a source S are on the same side of the throat. A light ray with an impact

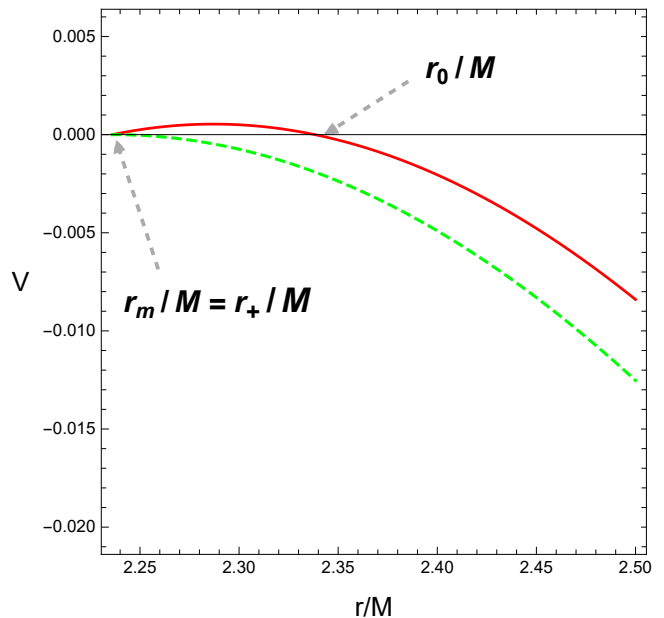


FIG. 3. Effective potentials V with $Q/M = 1.2$. A solid (red) curve denotes an effective potential V with $b/M = 1.01b_m/M = 4.09$ and $r_0/M = 2.34$, a dashed (green) curve denotes V with $b/m = b_m/m = 4.05$, and a dot-dashed (black) curve denotes V with $b/M = r_+^2/(r_+ - M) = 4.72$. Note $r_m/M = r_+/M = 2.24$.

parameter b is emitted by S with a source angle ϕ it is reflected with a deflection angle α by a wormhole as a lens L and it is observed by O as an image I with an image angle θ . We assume small angles $\bar{\alpha} \ll 1$, $\theta = b/D_{ol} \ll 1$, and $\phi \ll 1$, where D_{ol} is a distance between O and L and $\bar{\alpha}$ is an effective deflection angle of the light ray defined by

$$\bar{\alpha} \equiv \alpha \pmod{2\pi}. \quad (3.1)$$

We introduce the winding number N of the light, and we can express the deflection angle as

$$\alpha = \bar{\alpha} + 2\pi N. \quad (3.2)$$

The small-angle lens equation [69] is obtained from the lens configuration in Fig. 4 as

$$D_{ls} \bar{\alpha} = D_{os} (\theta - \phi), \quad (3.3)$$

where D_{ls} and $D_{os} = D_{ol} + D_{ls}$ are the distances between L and S and between O and S, respectively.

IV. GRAVITATIONAL LENSING UNDER A WEAK-FIELD APPROXIMATION

Under a weak-field approximation $r_m \ll r_0$ or $b_m \ll b$, by using $r_0 \sim b$, the deflection angle is given by

$$\alpha = 2 \left(M + \frac{Q^2}{M} \right) \frac{1}{b} = \frac{2(M+m)}{b}, \quad (4.1)$$

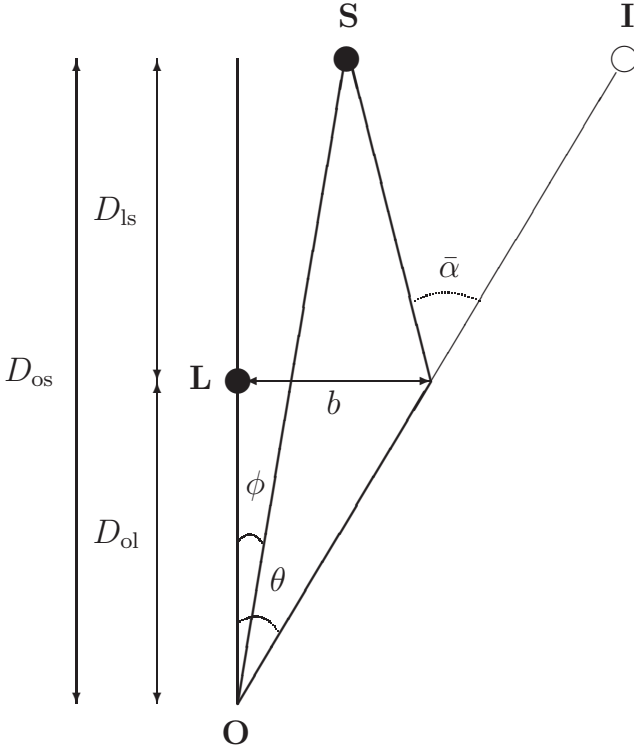


FIG. 4. Lens configuration. A source S with a source angle ϕ emits a light ray with an impact parameter b . It is reflected by a lens L with an effective deflection angle $\bar{\alpha}$ on a lens plane. An observer O sees it as an image I with an image angle θ . Note that S and O are the same side of a wormhole throat. The distances between O and S , between L and S , and between O and L are denoted by D_{os} , D_{ls} , and D_{ol} , respectively.

the winding number N must vanish, and the lens equation can be written in

$$\hat{\theta}^2 - \hat{\phi}^2 = 1, \quad (4.2)$$

where $\hat{\theta}$ and $\hat{\phi}$ are a reduced image angle and a reduced source angle defined by

$$\hat{\theta} \equiv \frac{\theta}{\theta_{E0}} \quad (4.3)$$

and

$$\hat{\phi} \equiv \frac{\phi}{\theta_{E0}}, \quad (4.4)$$

respectively, and where θ_{E0} is the image angle of an Einstein ring with $N = 0$ obtained as

$$\theta_{E0} \equiv \theta_{0+}(0) = \sqrt{\frac{2(M+m)D_{ls}}{D_{os}D_{ol}}}, \quad (4.5)$$

and the positive and negative solutions $\hat{\theta} = \hat{\theta}_{0\pm}$ of the lens equation with $N = 0$ is obtained as

$$\hat{\theta}_{0\pm}(\hat{\phi}) \equiv \frac{1}{2} \left(\hat{\phi} \pm \sqrt{\hat{\phi}^2 + 4} \right). \quad (4.6)$$

Here and hereinafter, the upper (lower) sign is chosen for the positive (negative) image angle or the positive (negative) impact parameter. The magnifications for the images are given by

$$\begin{aligned} \mu_{0\pm} &\equiv \frac{\hat{\theta}_{0\pm}}{\hat{\phi}} \frac{d\hat{\theta}_{0\pm}}{d\hat{\phi}} \\ &= \frac{1}{4} \left(2 \pm \frac{\hat{\phi}}{\sqrt{\hat{\phi}^2 + 4}} \pm \frac{\sqrt{\hat{\phi}^2 + 4}}{\hat{\phi}} \right) \end{aligned} \quad (4.7)$$

and its total magnification becomes

$$\begin{aligned} \mu_{\text{tot}} &\equiv |\mu_{0+}| + |\mu_{0-}| \\ &= \frac{1}{2} \left(\frac{\hat{\phi}}{\sqrt{\hat{\phi}^2 + 4}} + \frac{\sqrt{\hat{\phi}^2 + 4}}{\hat{\phi}} \right). \end{aligned} \quad (4.8)$$

V. DEFLECTION ANGLE IN A STRONG DEFLECTION LIMIT

We investigate the deflection angle of a ray in a strong deflection limit $b \rightarrow b_m$ in the following form:

$$\begin{aligned} \alpha &= -\bar{a} \log \left(\frac{b}{b_m} - 1 \right) + \bar{b} \\ &+ O \left(\left(\frac{b}{b_m} - 1 \right) \log \left(\frac{b}{b_m} - 1 \right) \right), \end{aligned} \quad (5.1)$$

where \bar{a} and \bar{b} are parameters.²

A. For $1 < Q/M < 2/\sqrt{3}$

In this case $1 < Q/M < 2/\sqrt{3}$, the photon sphere of a light ray with $b = b_m = 4M$ is at $r = r_m = 2M$. We introduce a variable [38]

$$z \equiv 1 - \frac{r_0}{r} \quad (5.2)$$

and we rewrite $I(r_0)$ as

$$I(r_0) = \int_0^1 R(z, r_0) F(z, r_0) dz, \quad (5.3)$$

where $R(z, r_0)$ is given by

$$R(z, r_0) \equiv \frac{2\sqrt{M}r_0}{\sqrt{M[r_0^2 + Q^2(1-z)^2] + 2Q^2r_0(z-1)}} \quad (5.4)$$

and $F(z, r_0)$ is defined by

$$F(z, r_0) \equiv \frac{1}{\sqrt{f(z, r_0)}}, \quad (5.5)$$

² We should read the order of a following term $O(b-b_m)$ in Ref. [5] as $O((b/b_m - 1) \log(b/b_m - 1))$ as discussed in Refs. [33, 35, 38].

where $f(z, r_0)$ is given by

$$f(z, r_0) \equiv \frac{r_0^4}{b^2(r_0) [r_0 + M(z-1)]^2} - (1-z)^2. \quad (5.6)$$

We expand $h(z, r_0)$ in power of z to obtain

$$f(z, r_0) = c_1(r_0)z + c_2(r_0)z^2 + O(z^3), \quad (5.7)$$

where $c_1(r_0)$ and $c_2(r_0)$ are given by

$$c_1(r_0) \equiv \frac{2(2M - r_0)}{M - r_0} \quad (5.8)$$

and

$$c_2(r_0) \equiv \frac{2M^2 + 2Mr_0 - r_0^2}{(M - r_0)^2}, \quad (5.9)$$

respectively. Here, we have used Eq. (2.10). From $c_{1m} \equiv c_1(r_m) = 0$ and $c_{2m} \equiv c_2(r_m) = 2$, $f(z, r_0)$ diverges in order of z^{-1} at $z \rightarrow 0$. By using

$$c_1(r_0) = c'_{1m}(r_0 - r_m) + O((r_0 - r_m)^2), \quad (5.10)$$

where $c'_{1m} = 2/M$, and

$$b(r_0) = b_m + \frac{1}{2}b''_m(r_0 - r_m)^2 + O((r_0 - r_m)^3), \quad (5.11)$$

where $b_m = 4M$ and $b''_m = 2/M$,

We separate I into a divergent part I_D and a regular part I_R . The divergent part is defined by

$$I_D = \int_0^1 R(0, r_m) F_D(z, r_0) dz, \quad (5.12)$$

where $R(0, r_m)$ is given by

$$R(0, r_m) = \frac{4M}{\sqrt{4M^2 - 3Q^2}} \quad (5.13)$$

and $F_D(z, r_0)$ is defined by

$$F_D(z, r_0) \equiv \frac{1}{\sqrt{c_1(r_0)z + c_2(r_0)z^2}}. \quad (5.14)$$

We can integrate I_D as [5, 38]

$$I_D = \frac{2R(0, r_m)}{\sqrt{c_2(r_0)}} \log \frac{\sqrt{c_2(r_0)} + \sqrt{c_1(r_0) + c_2(r_0)}}{\sqrt{c_1(r_0)}} \quad (5.15)$$

By using Eqs. (5.10)-(5.15), I_D in a strong deflection limit $r_0 \rightarrow r_m$ or $b \rightarrow b_m$ is obtained as

$$I_D = -\bar{a} \log \left(\frac{b}{b_m} - 1 \right) + \bar{a} \log 4, \quad (5.16)$$

where \bar{a} is given by

$$\bar{a} \equiv \frac{\sqrt{2}M}{\sqrt{4M^2 - 3Q^2}}. \quad (5.17)$$

Note that \bar{a} diverges in a limit $Q/M \rightarrow 2/\sqrt{3} - 0$. The regular part I_R is given by

$$I_R = \int_0^1 G(z, r_0) dz, \quad (5.18)$$

where $G(z, r_0)$ is defined as

$$G(z, r_0) \equiv R(z, r_0)F(z, r_0) - R(0, r_m)F_D(z, r_0). \quad (5.19)$$

We expand $G(z, r_0)$ in the power of $r_0 - r_m$ as

$$I_R(r_0) = \sum_{j=0}^{\infty} \frac{1}{j!} (r_0 - r_m)^j \int_0^1 \left. \frac{\partial^j G}{\partial r_0^j} \right|_{r_0=r_m} dz \quad (5.20)$$

and we consider the first term, in which we are interested,

$$I_R(r_0) = \int_0^1 G(z, r_m) dz. \quad (5.21)$$

We can express \bar{b} as

$$\bar{b} = +\bar{a} \log 4 + I_R - \pi. \quad (5.22)$$

The parameters \bar{a} and \bar{b} are shown in Fig. 5. In the

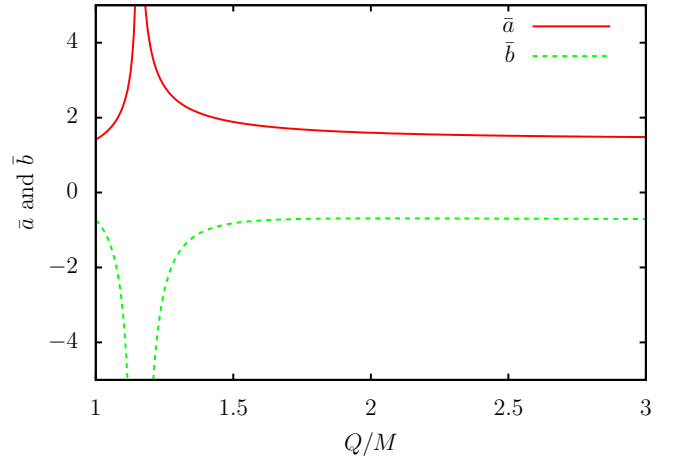


FIG. 5. Solid (red) and dashed (green) curves denote the parameters \bar{a} and \bar{b} in the deflection angles, respectively.

extreme charged Reissner-Nordström black hole limit $Q \rightarrow M$, the parameters are obtained analytically as $\bar{a} = \sqrt{2} \sim 1.41$ and $\bar{b} = \sqrt{2} \log [32(3 - 2\sqrt{2})] - \pi \sim -0.733$ as shown in Refs. [37, 38].

B. For $Q/M > 2/\sqrt{3}$

In the case of $Q/M > 2/\sqrt{3}$, there is a photon sphere with $b = b_m = r_+^2/(r_+ - M)$ on the throat at $r = r_m = r_+$. Since $R(0, r_m)$ diverges for $z = 0$, we express the divergent term I_D as

$$I(r_0) = \int_0^1 S(z, r_0) H(z, r_0) dz, \quad (5.23)$$

where $S(z, r_0)$ and $H(z, r_0)$ are defined by

$$S(z, r_0) \equiv 2\sqrt{M}r_0 [r_0 + M(z - 1)] \quad (5.24)$$

and

$$H(z, r_0) \equiv \frac{1}{\sqrt{h(z, r_0)}}, \quad (5.25)$$

respectively, where $h(z, r_0)$ is given by

$$h(z, r_0) \equiv \left\{ (M - r_0)^2 - (z - 1)^2 [M(z - 1) + r_0]^2 \right\} \\ \times \left\{ M [Q^2(z - 1)^2 + r_0^2] + 2Q^2r_0(z - 1) \right\}. \quad (5.26)$$

Here we have used $b(r_0) = r_0^2/(r_0 - M)$. We expand $h(z, r_0)$ in power of z as

$$h(z, r_0) = \bar{c}_1(r_0)z + \bar{c}_2(r_0)z^2 + O(z^3), \quad (5.27)$$

where $\bar{c}_1(r_0)$ and $\bar{c}_2(r_0)$ are given by

$$\bar{c}_1(r_0) \equiv 2(2M^2 - 3Mr_0 + r_0^2) [M(Q^2 + r_0^2) - 2Q^2r_0] \quad (5.28)$$

and

$$\bar{c}_2(r_0) \equiv -14M^3Q^2 + 6r_0^3(M^2 + Q^2) - Mr_0^4 \\ - Mr_0^2(6M^2 + 29Q^2) + 38M^2Q^2r_0, \quad (5.29)$$

respectively. Since we get $\bar{c}_{1m} \equiv \bar{c}_1(r_m) = 0$ and

$$\bar{c}_{2m} \equiv \bar{c}_2(r_m) = \frac{4Q^2(Q^2 - M^2)}{M^3} \\ \times \left[2M^4 - 7M^2Q^2 + (4Q^2 - 5M^2)Q\sqrt{Q^2 - M^2} + 4Q^4 \right], \quad (5.30)$$

$h(z, r_0)$ diverges in order of z^{-1} for $z = 0$. By using

$$\bar{c}_1(r_0) = \bar{c}'_{1m}(r_0 - r_m) + O((r_0 - r_m)^2), \quad (5.31)$$

where

$$\bar{c}'_{1m} = \frac{2(M^2 - Q^2)\sqrt{Q^2 - M^2} + 3M^2Q - 2Q^3}{M^2} \\ \times 4Q(M^2 - Q^2), \quad (5.32)$$

and

$$b(r_0) = b_m + b'_m(r_0 - r_m) + O((r_0 - r_m)^2), \quad (5.33)$$

where b'_m is given by

$$b'_m = \frac{Q^2 - 2Q\sqrt{Q^2 - M^2}}{M^2 - Q^2}. \quad (5.34)$$

In the case, I is separated into a divergent part I_d and a regular part I_r . The divergent part is defined by

$$I_d \equiv \int_0^1 S(0, r_m)H_d(z, r_0)dz, \quad (5.35)$$

where $S(0, r_m)$ is obtained as

$$S(0, r_m) = \frac{2Q\sqrt{Q^2 - M^2}(\sqrt{Q^2 - M^2} + Q)^2}{M^{3/2}} \quad (5.36)$$

and $H_d(z, r_0)$ is defined by

$$H_d(z, r_0) \equiv \frac{1}{\sqrt{\bar{c}_1(r_0)z + \bar{c}_2(r_0)z^2}}. \quad (5.37)$$

The divergent term I_d can be integrated as [5, 38]

$$I_d = \frac{2S(0, r_m)}{\sqrt{\bar{c}_2(r_0)}} \log \frac{\sqrt{\bar{c}_2(r_0)} + \sqrt{\bar{c}_1(r_0) + \bar{c}_2(r_0)}}{\sqrt{\bar{c}_1(r_0)}} \quad (5.38)$$

From Eqs. (5.31)-(5.38), I_d in a strong deflection limit $r_0 \rightarrow r_m$ or $b \rightarrow b_m$ is given by

$$I_d = -\bar{a} \log \left(\frac{b}{b_m} - 1 \right) + \bar{a} \log \frac{8\sqrt{Q^2 - M^2} - 4Q}{\sqrt{Q^2 - M^2}}, \quad (5.39)$$

where \bar{a} is obtained as

$$\bar{a} = \frac{(Q + \sqrt{Q^2 - M^2})^2}{\sqrt{2M^4 - 7M^2Q^2 + 4Q^4 + (4Q^2 - 5M^2)Q\sqrt{Q^2 - M^2}}}. \quad (5.40)$$

Notice that \bar{a} diverges in a limit $Q/M \rightarrow 2/\sqrt{3} + 0$.

We define the regular part I_r as

$$I_r \equiv \int_0^1 g(z, r_0)dz, \quad (5.41)$$

where $g(z, r_0)$ is given by

$$g(z, r_0) \equiv S(z, r_0)H(z, r_0) - S(0, r_m)H_d(z, r_0) \quad (5.42)$$

and it can be expanded in the power of $r_0 - r_m$ as

$$I_r(r_0) = \sum_{j=0}^{\infty} \frac{1}{j!} (r_0 - r_m)^j \int_0^1 \frac{\partial^j g}{\partial r_0^j} \Big|_{r_0=r_m} dz \quad (5.43)$$

and the first term is given by,

$$I_r(r_0) = \int_0^1 g(z, r_m)dz. \quad (5.44)$$

Thus, we can express \bar{b} as

$$\bar{b} = \bar{a} \log \frac{8\sqrt{Q^2 - M^2} - 4Q}{\sqrt{Q^2 - M^2}} + I_r - \pi. \quad (5.45)$$

Notice that \bar{a} and \bar{b} are shown in Fig. 5. The ultrastatic limit $M \rightarrow 0$ under the fixed ADM mass m , the deflection angle of the ray is obtained as $\bar{a} = \sqrt{2} \sim 1.41$ and $\bar{b} = 2\sqrt{2} \log [4(2 - \sqrt{2})] - \pi = \sqrt{2} \log [32(3 - 2\sqrt{2})] - \pi \sim -0.733$ as shown by Tsukamoto and Harada [6]. Notice that the parameters \bar{a} and \bar{b} are coincident with the ones in the case of $Q \rightarrow M$.

VI. OBSERVABLES IN A STRONG DEFLECTION LIMIT

We introduce an angle θ_N^0 defined by

$$\alpha(\theta_N^0) = 2\pi N \quad (6.1)$$

and we expand the effective deflection angle $\alpha(\theta)$ around $\theta = \theta_N^0$ to obtain

$$\alpha(\theta) = \alpha(\theta_N^0) + \left. \frac{d\alpha}{d\theta} \right|_{\theta=\theta_N^0} (\theta - \theta_N^0) + O((\theta - \theta_N^0)^2). \quad (6.2)$$

In the strong deflection limit $b \rightarrow b_m + 0$, the deflection angle is expressed by

$$\begin{aligned} \alpha(\theta) = & -\bar{a} \log \left(\frac{\theta}{\theta_\infty} - 1 \right) + \bar{b} \\ & + O \left(\left(\frac{\theta}{\theta_\infty} - 1 \right) \log \left(\frac{\theta}{\theta_\infty} - 1 \right) \right), \end{aligned} \quad (6.3)$$

where $\theta_\infty \equiv b_m/D_{o1}$ is image angle of the photon sphere, and θ_N^0 is obtained as, from Eqs. (6.1) and (6.3),

$$\theta_N^0 = \left(1 + e^{\frac{\bar{b}-2\pi N}{\bar{a}}} \right) \theta_\infty \quad (6.4)$$

and we obtain, from Eq. (6.3),

$$\left. \frac{d\alpha}{d\theta} \right|_{\theta=\theta_N^0} = \frac{\bar{a}}{\theta_\infty - \theta_N^0} \quad (6.5)$$

and the effective deflection angle for the positive solution $\theta = \theta_N$ of the lens equation with a positive winding number N is given by, from Eqs. (3.2), (6.1), (6.2), (6.4), and (6.5),

$$\bar{\alpha}(\theta_N) = \frac{\bar{a}}{\theta_\infty e^{\frac{\bar{b}-2\pi N}{\bar{a}}}} (\theta_N^0 - \theta_N). \quad (6.6)$$

By substitute the effective deflection angle (6.6) into the lens equation (3.3), we obtain the positive solution of the lens equation or the image angle for the positive winding number N as

$$\theta_N(\phi) \sim \theta_N^0 - \frac{\theta_\infty e^{\frac{\bar{b}-2\pi N}{\bar{a}}} D_{os} (\theta_N^0 - \phi)}{\bar{a} D_{ls}}, \quad (6.7)$$

and the radius of an Einstein ring with the positive winding number N as

$$\theta_{EN} \equiv \theta_N(0) \sim \left(1 - \frac{\theta_\infty e^{\frac{\bar{b}-2\pi N}{\bar{a}}} D_{os}}{\bar{a} D_{ls}} \right) \theta_N^0, \quad (6.8)$$

and the difference between the outermost image angle and the innermost one \bar{s} as

$$\bar{s} \equiv \theta_1 - \theta_\infty \sim \theta_1^0 - \theta_\infty^0 = \theta_\infty e^{\frac{\bar{b}-2\pi}{\bar{a}}}. \quad (6.9)$$

The magnification of the image with $\theta_N(\phi)$ for each positive winding number N is given by

$$\mu_N \equiv \frac{\theta_N}{\phi} \frac{d\theta_N}{d\phi} \sim \frac{\theta_\infty^2 D_{os} \left(1 + e^{\frac{\bar{b}-2\pi N}{\bar{a}}} \right) e^{\frac{\bar{b}-2\pi N}{\bar{a}}}}{\phi \bar{a} D_{ls}}, \quad (6.10)$$

and the sum of the magnification from $N = 1$ to ∞ is given by

$$\sum_{N=1}^{\infty} \mu_N \sim \frac{\theta_\infty^2 D_{os} \left(1 + e^{\frac{2\pi}{\bar{a}}} + e^{\frac{\bar{b}}{\bar{a}}} \right) e^{\frac{\bar{b}}{\bar{a}}}}{\phi \bar{a} D_{ls} \left(e^{\frac{4\pi}{\bar{a}}} - 1 \right)}, \quad (6.11)$$

and the ratio of the magnification of the outermost images to the others \bar{r} is given by

$$\bar{r} \equiv \frac{\mu_1}{\sum_{N=2}^{\infty} \mu_N} \sim \frac{\left(e^{\frac{4\pi}{\bar{a}}} - 1 \right) \left(e^{\frac{2\pi}{\bar{a}}} + e^{\frac{\bar{b}}{\bar{a}}} \right)}{e^{\frac{2\pi}{\bar{a}}} + e^{\frac{4\pi}{\bar{a}}} + e^{\frac{\bar{b}}{\bar{a}}}}, \quad (6.12)$$

where $\sum_{N=2}^{\infty} \mu_N$ is

$$\sum_{N=2}^{\infty} \mu_N \sim \frac{\theta_\infty^2 D_{os} \left(e^{\frac{2\pi}{\bar{a}}} + e^{\frac{4\pi}{\bar{a}}} + e^{\frac{\bar{b}}{\bar{a}}} \right) e^{\frac{\bar{b}-4\pi}{\bar{a}}}}{\phi \bar{a} D_{ls} \left(e^{\frac{4\pi}{\bar{a}}} - 1 \right)}. \quad (6.13)$$

VII. DISCUSSION AND CONCLUSION

We have investigated the gravitational lensing by the Bronnikov-Kim wormhole under the weak-field approximation and in the strong deflection limit. the Bronnikov-Kim wormhole metric is the same as the one of a wormhole filled with massless and neutral fermions in Einstein-Dirac-Maxwell theory in a simple case [58, 59]. The metric becomes the one of an extreme charged Reissner-Nordström black hole in a limit $Q \rightarrow M$ and the one of a spatial Schwarzschild wormhole [55] in an ultrastatic limit $M \rightarrow 0$ under a constant ADM mass m . The parameter \bar{b} of the Bronnikov-Kim wormhole has been calculated in numerical partly while \bar{b} of the extreme charged Reissner-Nordström black hole [37, 38] and the spatial Schwarzschild wormhole [6] are obtained in analytical. Interestingly, in the both cases for the extreme charged Reissner-Nordström black hole and the spatial Schwarzschild wormhole, we obtain exactly the same parameters $\bar{a} = \sqrt{2}$ and $\bar{b} = \sqrt{2} \log [32(3 - 2\sqrt{2})] - \pi$.

Recently, In Ref. [64], Jusufi *et al.* have discussed shadow images under an assumption that a supermassive compact object at the center of our galaxy is the Bronnikov-Kim wormhole and, from observational data on the orbit of S2 star [70], they have concluded that the parameters of the metric $Q \sim 8 \times 10^6 M_\odot$ and $M \sim 4 \times 10^6 M_\odot$. Note that a Schwarzschild black hole with an ADM mass $m_S = 4 \times 10^6 M_\odot$, which matches the observation of orbit of S2 star, can form an Einstein ring with a diameter $2\theta_{E0} \sim 2.86$ arcsecond and a photon sphere with a diameter $2\theta_\infty \sim 51.58 \mu\text{as}$ if we set distances $D_{os} = 16$ kpc and $D_{o1} = D_{ls} = 8$ kpc as

shown Appendix B. On the other hand, the Bronnikov-Kim wormhole with the parameters $Q = 8 \times 10^6 M_\odot$ and $M = 4 \times 10^6 M_\odot$ has $2\theta_{E0} \sim 4.52$ arcsecond and $2\theta_\infty \sim 85.56 \mu\text{as}$ as shown Table I. Therefore, we would distinguish the Schwarzschild black hole with and ADM mass $m_S = 4 \times 10^6 M_\odot$ and the Bronnikov-Kim wormhole with the parameters $Q \sim 8 \times 10^6 M_\odot$ and $M \sim 4 \times 10^6 M_\odot$ at the center of our galaxy if lensed images under the weak-field approximation and D_{ol} are observed or if lensed images in the strong deflection limit are observed.

On this paper, we do not treat the gravitational lensing by the marginally unstable photon sphere on the throat with $Q/M = 2/\sqrt{3}$ since the deflection angle would diverge nonlogarithmically as well as Ref. [22] or Ref. [23].

Appendix A: Arnowitt-Deser-Misner (ADM) mass

We calculate an Arnowitt-Deser-Misner (ADM) mass [71]. Under the weak-field approximation, the line element

$$\begin{aligned} ds^2 &= -\left(1 - \frac{2M}{r}\right) dt^2 \\ &\quad + \left(1 + \frac{2Q^2}{Mr}\right) dr^2 + r^2(d\vartheta^2 + \sin^2\vartheta d\varphi^2) \\ &= -\left(1 - \frac{2M}{r(r_*)}\right) dt^2 \\ &\quad + \left(1 + \frac{2Q^2}{Mr_*}\right) [dr_*^2 + r_*^2(d\vartheta^2 + \sin^2\vartheta d\varphi^2)] \end{aligned} \quad (\text{A1})$$

We consider a hypersurface Σ_t which is the surface of constant t and a unit normal to the hypersurface Σ_t is given by $n_\mu = -(1 - M/r)\partial_t$ and a induced metric on the hypersurface is given by

$$h_{ab}dy^a dy^b = \left(1 + \frac{2Q^2}{Mr_*}\right) [dr_*^2 + r_*^2(d\vartheta^2 + \sin^2\vartheta d\varphi^2)]. \quad (\text{A2})$$

Its boundary S_t is a two-sphere $r_* = R_*$ and its unit normal is given by

$$r_{*a} = \left(1 + \frac{Q^2}{Mr_*}\right) \partial_{r_*} \quad (\text{A3})$$

and an induced metric on the boundary S_t is given by

$$\sigma_{AB}d\theta^A d\theta^B = \left(1 + \frac{2Q^2}{MR_*}\right) R_*^2(d\vartheta^2 + \sin^2\vartheta d\varphi^2). \quad (\text{A4})$$

The ADM mass m is obtained as

$$m \equiv -\frac{1}{8\pi} \lim_{S_t \rightarrow \infty} \oint_{S_t} (k - k_0) \sqrt{\sigma} d^2\theta = \frac{Q^2}{M}, \quad (\text{A5})$$

where the extrinsic curvature of S_t embedded in Σ_t is given by

$$k = r_{*|a}^a = \frac{2}{R_*} \left(1 - \frac{2Q^2}{MR_*}\right), \quad (\text{A6})$$

the extrinsic curvature of S_t embedded in a flat space is given by

$$k_0 = \frac{2}{\left(1 + \frac{2Q^2}{MR_*}\right)^{1/2} R_*} = \frac{2}{R_*} \left(1 - \frac{Q^2}{MR_*}\right), \quad (\text{A7})$$

and the leading term of σ is given by $\sigma = R_*^4 \sin^2\vartheta$.

Appendix B: Schwarzschild Lens

The line element in the Schwarzschild spacetime is given by

$$ds^2 = -\left(1 - \frac{2m_S}{r}\right) dt^2 + \frac{dr^2}{\left(1 - \frac{2m_S}{r}\right)} + r^2(d\vartheta^2 + \sin^2\vartheta d\varphi^2), \quad (\text{B1})$$

where m_S is the ADM mass of a black hole or a lens. The deflection angle of a ray under the weak-field approximation is obtained as

$$\alpha \sim \frac{4m_S}{b} \quad (\text{B2})$$

and the radius of an Einstein ring is given by

$$\theta_{E0} \equiv \theta_{0+}(0) = \sqrt{\frac{4m_S D_{\text{ls}}}{D_{\text{os}} D_{\text{ol}}}}. \quad (\text{B3})$$

In the strong deflection limit, we obtain $\bar{a} = 1$ and $\bar{b} = \log[216(7 - 4\sqrt{3})] - \pi \sim -0.40$ are obtained in Refs. [5, 9, 16, 33]

For a supermassive compact object at the center of our galaxy, we set the ADM mass $m_S = 4 \times 10^6 M_\odot$, distances $D_{\text{os}} = 16$ kpc and $D_{\text{ol}} = D_{\text{ls}} = 8$ kpc and we obtain the diameters of the Einstein ring $2\theta_{E0} \sim 2.86$ arcsecond and the photon sphere $2\theta_\infty \sim 51.58 \mu\text{as}$.

-
- [1] P. Schneider, J. Ehlers, and E. E. Falco, *Gravitational Lenses* (Springer-Verlag, Berlin, 1992).
 [2] P. Schneider, C. S. Kochanek, and J. Wambsganss, *Gravitational Lensing: Strong, Weak and Micro*, *Lecture Notes of the 33rd Saas-Fee Advanced Course*, edited by

- G. Meylan, P. Jetzer, and P. North (Springer-Verlag, Berlin, 2006).
 [3] B. P. Abbott *et al.* [LIGO Scientific and Virgo Collaborations], *Phys. Rev. Lett.* **116**, 061102 (2016).
 [4] K. Akiyama *et al.* [Event Horizon Telescope Collabora-

TABLE I. Parameters \bar{a} and \bar{b} , the diameters of the photon sphere $2\theta_\infty$ and the the outermost image $2\theta_{E1}$, their difference of their radii $\bar{s} = \theta_{E1} - \theta_\infty$, the magnification of the pair of the outermost images $\mu_{1\text{tot}}(\phi) \sim 2|\mu_1|$, the ratio of the magnification of the outermost image to the others $\bar{r} = \mu_1 / \sum_{N=2}^{\infty} \mu_N$, and the diameter of an Einstein ring $2\theta_{E0}$ for given Q/M are shown. We set the parameter $M = 4 \times 10^6 M_\odot$, distances $D_{\text{os}} = 16$ kpc and $D_{\text{o1}} = D_{\text{ls}} = 8$ kpc and the source angle $\phi = 1$ arcsecond.

Q/M	1	1.1	1.2	1.5	1.8	2	2.2	2.5	3
\bar{a}	1.41	2.33	3.84	1.89	1.66	1.60	1.56	1.52	1.48
\bar{b}	-0.733	-3.312	-6.150	-0.820	-0.698	-0.689	-0.690	-0.696	-0.705
$2\theta_\infty$ [μas]	39.71	39.71	40.15	52.30	70.84	85.56	102.0	129.7	184.1
$2\theta_{E1}$ [μas]	40.00	40.35	41.72	53.51	71.91	86.64	103.1	131.0	185.7
\bar{s} [μas]	0.14	0.32	0.76	0.60	0.53	0.54	0.57	0.61	0.82
$\mu_{1\text{tot}}(\phi) \times 10^{17}$	3.8	5.4	8.3	17	22	29	37	55	100
\bar{r}	85	14	4.3	28	43	51	56	63	69
$2\theta_{E0}$ [arcsecond]	2.86	3.01	3.16	3.65	4.17	4.52	4.89	5.45	6.40

- tion], *Astrophys. J.* **875**, L1 (2019).
- [5] V. Bozza, *Phys. Rev. D* **66**, 103001 (2002).
- [6] N. Tsukamoto and T. Harada, *Phys. Rev. D* **95**, 024030 (2017).
- [7] V. Perlick, *Living Rev. Relativity* **7**, 9 (2004).
- [8] Y. Hagihara, *Jpn. J. Astron. Geophys.*, **8**, 67 (1931).
- [9] C. Darwin, *Proc. R. Soc. Lond. A* **249**, 180 (1959).
- [10] R. d' E. Atkinson, *Astron. J.* **70**, 517 (1965).
- [11] J.-P. Luminet, *Astron. Astrophys.* **75**, 228 (1979).
- [12] H. C. Ohanian, *Am. J. Phys.* **55**, 428 (1987).
- [13] R. J. Nemiroff, *Am. J. Phys.* **61**, 619 (1993).
- [14] S. Frittelli, T. P. Kling, and E. T. Newman, *Phys. Rev. D* **61**, 064021 (2000).
- [15] K. S. Virbhadra and G. F. R. Ellis, *Phys. Rev. D* **62**, 084003 (2000).
- [16] V. Bozza, S. Capozziello, G. Iovane, and G. Scarpetta, *Gen. Relativ. Gravit.* **33**, 1535 (2001).
- [17] V. Perlick, *Phys. Rev. D* **69**, 064017 (2004).
- [18] K. S. Virbhadra, *Phys. Rev. D* **79**, 083004 (2009).
- [19] V. Bozza, *Gen. Relativ. Gravit.* **42**, 2269 (2010).
- [20] R. Shaikh, P. Banerjee, S. Paul, and T. Sarkar, *JCAP* **1907**, 028 (2019).
- [21] R. Shaikh, P. Banerjee, S. Paul, and T. Sarkar, *Phys. Rev. D* **99**, 104040 (2019).
- [22] N. Tsukamoto, *Phys. Rev. D* **101**, 104021 (2020).
- [23] N. Tsukamoto, *Phys. Rev. D* **102**, 104029 (2020).
- [24] S. Paul, *Phys. Rev. D* **102**, 064045 (2020).
- [25] V. Bozza, *Phys. Rev. D* **67**, 103006 (2003).
- [26] E. F. Eiroa, G. E. Romero, and D. F. Torres, *Phys. Rev. D* **66**, 024010 (2002).
- [27] A. O. Petters, *Mon. Not. Roy. Astron. Soc.* **338**, 457 (2003).
- [28] E. F. Eiroa and D. F. Torres, *Phys. Rev. D* **69**, 063004 (2004).
- [29] V. Bozza and L. Mancini, *Astrophys. J.* **611**, 1045 (2004).
- [30] V. Bozza, F. De Luca, G. Scarpetta, and M. Sereno, *Phys. Rev. D* **72**, 083003 (2005).
- [31] V. Bozza and M. Sereno, *Phys. Rev. D* **73**, 103004 (2006).
- [32] V. Bozza, F. De Luca, and G. Scarpetta, *Phys. Rev. D* **74**, 063001 (2006).
- [33] S. V. Iyer and A. O. Petters, *Gen. Rel. Grav.* **39**, 1563 (2007).
- [34] V. Bozza and G. Scarpetta, *Phys. Rev. D* **76**, 083008 (2007).
- [35] N. Tsukamoto, *Phys. Rev. D* **94**, 124001 (2016).
- [36] A. Ishihara, Y. Suzuki, T. Ono, and H. Asada, *Phys. Rev. D* **95**, 044017 (2017).
- [37] N. Tsukamoto and Y. Gong, *Phys. Rev. D* **95**, 064034 (2017).
- [38] N. Tsukamoto, *Phys. Rev. D* **95**, 064035 (2017).
- [39] N. Tsukamoto, *Phys. Rev. D* **95**, 084021 (2017).
- [40] G. F. Aldi and V. Bozza, *JCAP* **02**, 033 (2017).
- [41] T. Hsieh, D. S. Lee, and C. Y. Lin, *Phys. Rev. D* **103**, 104063 (2021).
- [42] K. Takizawa and H. Asada, *Phys. Rev. D* **103**, 104039 (2021).
- [43] N. Tsukamoto, *Phys. Rev. D* **103**, 024033 (2021).
- [44] N. Tsukamoto, [arXiv:2105.14336 [gr-qc]].
- [45] F. Aratore and V. Bozza, [arXiv:2107.05723 [gr-qc]].
- [46] E. F. Eiroa, *Phys. Rev. D* **71**, 083010 (2005).
- [47] M. Visser, *Lorentzian Wormholes: From Einstein to Hawking* (American Institute of Physics, Woodbury, NY, 1995).
- [48] T. Damour and S. N. Solodukhin, *Phys. Rev. D* **76**, 024016 (2007).
- [49] J. P. S. Lemos and O. B. Zaslavskii, *Phys. Rev. D* **78**, 024040 (2008).
- [50] N. Tsukamoto and T. Kokubu, *Phys. Rev. D* **101** 044030 (2020).
- [51] M. S. Morris and K. S. Thorne, *Am. J. Phys.* **56**, 395 (1988).
- [52] H. G. Ellis, *J. Math. Phys.* **14**, 104 (1973).
- [53] K. A. Bronnikov, *Acta Phys. Pol. B* **4**, 251 (1973).
- [54] C. Martinez and M. Nozawa, *Phys. Rev. D* **103**, 024003 (2021).
- [55] N. Dadhich, S. Kar, S. Mukherji, and M. Visser, *Phys. Rev. D* **65**, 064004 (2002).
- [56] K. A. Bronnikov and S. W. Kim, *Phys. Rev. D* **67**, 064027 (2003).
- [57] K. A. Bronnikov, V. N. Melnikov, and H. Dehnen, *Phys. Rev. D* **68**, 024025 (2003).
- [58] J. L. Blázquez-Salcedo, C. Knoll and E. Radu, *Phys. Rev. Lett.* **126**, 101102 (2021).
- [59] K. Bronnikov, S. Bolokhov, S. Krasnikov and M. Skvortsova, [arXiv:2104.10933 [gr-qc]].
- [60] J. L. Blázquez-Salcedo, C. Knoll and E. Radu,

- [arXiv:2108.12187 [gr-qc]].
- [61] D. L. Danielson, G. Satishchandran, R. M. Wald and R. J. Weinbaum, [arXiv:2108.13361 [gr-qc]].
- [62] R. A. Konoplya and A. Zhidenko, [arXiv:2106.05034 [gr-qc]].
- [63] K. A. Bronnikov, R. A. Konoplya, and T. D. Pappas, Phys. Rev. D **103**, 124062 (2021).
- [64] K. Jusufi, S. K., M. Azreg-Aïnou, M. Jamil, Q. Wu, and C. Bambi, [arXiv:2106.08070 [gr-qc]].
- [65] M. S. Churilova, R. A. Konoplya, Z. Stuchlik and A. Zhidenko, JCAP **10**, 010 (2021).
- [66] J. Keir, Class. Quant. Grav. **33**, 135009 (2016).
- [67] V. Cardoso, L. C. B. Crispino, C. F. B. Macedo, H. Okawa, and P. Pani, Phys. Rev. D **90**, 044069 (2014).
- [68] P. V. P. Cunha, E. Berti, and C. A. R. Herdeiro, Phys. Rev. Lett. **119**, 251102 (2017).
- [69] V. Bozza, Phys. Rev. D **78**, 103005 (2008).
- [70] T. Do, A. Hees, A. Ghez, G. D. Martinez, D. S. Chu, S. Jia, S. Sakai, J. R. Lu, A. K. Gautam and K. K. O’Neil, *et al.* Science **365**, no.6454, 664-668 (2019).
- [71] E. Poisson, *A Relativist’s Toolkit: The Mathematics of Black-Hole Mechanics*, (Cambridge University Press, Cambridge, 2004).